Antibacterial properties of bioactive glass particle abraded titanium against *Streptococcus mutans*

Faleh Abushahba[1], Eva Söderling[1], Laura Aalto-Setälä[2], Johan Sangder[2], Leena Hupa[2], Timo O. Närhi[1]

[1] Department of Prosthetic Dentistry and Stomatognathic Physiology, Institute of Dentistry, University of Turku, Finland

[2] Johan Gadolin Process Chemistry Centre, Åbo Akademi University, Turku, Finland

Abstract

The purpose of this study was to evaluate effects of titanium surfaces air-abraded with particles of Bioglass® 45S5 and three-ZnO and SrO doped compositions on the viability, adhesion and biofilm formation of *Streptococcus mutans.*

A statistically significant decrease in the viability of *S. mutans* was observed for all titanium discs air-particle abraded with the BAGs ($p<0.001$). Also, a significant effect on diminishing biofilm formation on the titanium discs was seen for all BAGs ($p<0.01$). No differences were noticed in *S. mutans* adhesion on titanium surfaces treated with different glasses ($p = 0.964$). Static SBF immersion experiments showed that after 2 and 48 h the BAG doped with 4 mol% ZnO demonstrated the highest Zn^{2+} ion concentration released into SBF (0.2 mg/L). 45S5 BAG demonstrated the highest statistically significant increase in the pH throughout the 120 min of static immersion ($p<0.001$).

In conclusion, we showed that titanium alloy discs abraded with particles of the experimental compositions and 45S5 BAG had strong antimicrobial activity against *S. mutans* and they suppressed *S. mutans* biofilm formation. The antimicrobial activity of 45S5 BAG was attributed to high pH whereas for the Zn-containing BAGs antimicrobial activity was due to steady release of Zn^{2+} into the interfacial solution.

Key words: Air-particle abrasion, bioactive glass, biofilm, titanium, *S. mutans*

INTRODUCTION

The use of oral implants is a widely accepted treatment modality with a predictable survival rate [1,2]. However, peri-implant disease may occur over time, which decreases the ultimate success of implant treatment [3]. It is due to the result of bone loss around the implant and subsequent loss of osseointegration [4]. Peri-implantitis is described as an infectious disease with many features in common with periodontitis [5]. It has been reported in 28% to 56% of patients, and in 12% to 43% in individual implants [6].

The adherence and proliferation of potential pathogenic bacteria on titanium implant surface has been associated to peri-implant disease occurrence [7]. Formation and establishment of subgingival microbiota around the implant is mainly dependent on continuous colonization of various bacterial species on the implant surface [8]. Biofilm formation on the implant surface is initiated by the adhesion of first gram positive bacterial colonizers [9]. Each of these bacterial species is believed to further facilitate the titanium surface colonization by the next bacterial colonizers, leading to the establishment of an anaerobic Gram-negative microbial environment [10,11].

The oral streptococci are members of the indigenous microbiota [12] and are considered the pioneer colonizers and might participate in the process, which can lead to implant failure on the long term [13]. The pathogenicity of *S. mutans* is mainly associated with its ability to form biofilm and produce an insoluble polymer matrix with a high affinity for solid surfaces such as tissue or implants [14]. Studies indicated that *S. mutans* isolates have a substantial ability to form biofilm and survive at low pH values that are toxic to most other bacteria [15].

Bioactive glasses (BAGs) were first introduced in the early 1970s by Hench and his co-workers. 45S5 BAG (SiO_2-Na_2O-P_2O_5-CaO) has shown the capability of forming direct chemical bonds with hard and soft tissue [16]. BAG is used clinically mainly in bone repair and regeneration, including orthopedics applications, periodontal pocket reduction, alveolar ridge augmentation and maxillofacial reconstruction [17]. S53P4 BAG, consisting of the same oxides but in different ratios than the 45S5 BAG, has previously been shown to have an antibacterial effect against some oral microorganisms [18]. Antibacterial activity of BAG is mainly attributed to high pH and osmotic effects caused by the nonphysiological concentrations of silica, sodium and calcium ions dissolved from the glass [18,19]. S53P4 BAG powder has shown a broad antibacterial effects on *A Actinomycetomcomitams*, *P. gingivalis, S. mutans* and *A. naeslundii* [18]. In addition, S53P4 has been show to induce clear antibacterial effects on in total 29 aerobic and 17 anaerobic bacteria species of clinical relevance [20,21]. Particulate 45S5 BAG has shown a considerable antibacterial effect against certain oral bacteria including supra- and subgingival bacteria [19] and has the prospective ability to reduce the bacterial colonization and biofilm formation [22].

ZnO has been considerably used as an antibacterial agent in dental applications such as root canal sealers, pulp capping liner and temporary fillers. Antibacterial activity of ZnO has been explained by several mechanisms. One of the mechanisms is the release of H_2O_2 which can penetrate the cell membrane and subsequently kill the bacteria [23]. Also Zn^{2+} ion can penetrate into the bacterial cells and produce toxic reactive oxygen species (ROS) [24] which subsequently lead to bacterial death. A recent study demonstrated that ZnO antibacterial activity against *S. mutans* could be attributed to

the release of Zn^{2+} ion which causes interruption of protein synthesis and interference with DNA replication [25]. In addition zinc has been known to encourage attachment and proliferation of osteoblast as well as inhibit osteoclastic cell and also being involved in calcification mechanism [26,27]. Numerous studies have shown that Sr^{2+} *in vitro* stimulates osteoblastic differentiation and bone nodule formation, promotes the type I collagen protein levels and inhibits the differentiation and activity of osteoclasts [28-31]. Recently, Sr^{2+} substituted bioactive glasses were reported to show antimicrobial effects on *A. actinomycetemcomitans* and *P. gingivalis* [32]. The several research efforts of doping bioactive glasses with Zn^{2+} have been summarized by Balasubramanian *et al*. (2015). In general, the known antibacterial activity is one of the main reasons to dope bioactive glasses with Zn^{2+}. ZnO enters the glass strcture either as a network modifier or as an intermediate oxide depening on the overall composition and total content of ZnO [33].

The purpose of this *in vitro* study was to evaluate *S. mutans* viability, adhesion and biofilm-effects related to changes in pH and levels of ions released from titanium surface after air-blasting with particles of BAG 45S5 and experimental BAGs doped with ZnO and SrO. The antibacterial effect of the glasses was compared with their ion dissolution kinetics in vitro. BAG 45S5 with known antibacterial activity and an inert, commercial alumino borosilicate glass (E-glass) served as a references.

MATERIALS AND METHODS

Abrasive glass preparation

The experimental glasses were based on molar substitution of ZnO and SrO for CaO and SiO_2 in the BAG 45S5 composition. The oxide compositions and codes of the glasses are given in table 1. In Zn4, 4 mol% ZnO was substituted for 2 mol% of both CaO and SiO_2, thus decreasing the calculated network connectivity from NC=2.12 for 45S5 to NC=1.94 for Zn4 (Table 1). In Zn6, the whole amount of ZnO was substituted for the network forming oxide SiO_2. This decreased the network connectivity to NC=1.54. In BAG Zn4Sr8, 4 mol% of ZnO and 8 mol% of SrO were substituted for 2 mol% of SiO_2 and 8 mol% of CaO, thus giving NC=1.95. The experimental BAGs and 45S5 BAG were melted in-house. Batches giving 300 g glass were mixed of analytical grade chemical Na_2CO_3 (Sigma-Aldrich), $CaHPO_4{\cdot}2H_2O$, $SrCO_3$, ZnO (all from Sigma-Aldrich), $CaCO_3$ (Fluka), H_3BO_3(Merck), and Belgian quartz sand for SiO_2. The glasses were melted in an uncovered platinum crucible at 1360ºC for 3 h in air. After casting, the received glass blocks were annealed at 520ºC for 1 h and then slowly cooled in the oven using our procedure for typical silicate –based bioactive glasses [34]. The blocks were crushed and re-melted to ensure homogeneity. The annealed blocks were crushed and sieved to give particles of the size range fractions 25-120µm and 300-500µm. The particle morphology was examined with a scanning electron microscope (SEM, Jeol-JSM 5500, Japan). Commercial alumino borosilicate glass (E-glass cullets) was used as inert referens.

Table 1 Nominal composition (mol.%) 45S5 and experimental BAGs. Network connectivity (NC) for the BAGs was calculated according to Hill and Brauer (2011) [35].

Glass Code	SiO_2	Na_2O	P_2O_5	CaO	ZnO	SrO	NC
45S5	46.1	24.3	2.6	26.9			2.12
Zn4	44.1	24.3	2.6	24.9	4.0		1.94
Zn6	40.1	24.3	2.6	26.9	6.0		1.54
Zn4Sr8	44.2	24.5	2.6	16.6	4.0	8.0	1.95

In vitro static SBF testing of the glasses:

The *in vitro* bioactivity of the BAGs was tested both in static and dynamic simulated body fluid, SBF. In the static ion dissolution tests, the particles (300-500 μm) were immersed in the SBF using the concentration 100 mg/mL. The particles were washed several times in acetone using an ultrasonic batch to remove any traces of fine grained powder adhered to the particle surfaces. The SBF was prepared according to the protocol by Kokubo et al. [36]. The sample containers were placed in a shaking incubator (rotation speed 120 rpm) at 37ºC for 48 h. After the immersion, the particles were separated from the fluid, and the reaction of the particles with the solution was stopped by careful washing with acetone and drying in an oven at 40ºC. The concentrations of the ions dissolved from the BAGs were measured for the solutions diluted in the ration 1:10 using inductively coupled plasma-atomic emission spectrometer (ICP-OES, Optima 5300 DV, Perkin Elmer). This dilution was taken into account when reporting the final values of the ion dissolution. Finally, the pH of the solution was measured. Additional pH measurements using the concentration 10 mg glass particles (300-500μm) to 4 mL SBF were done in order to better mimick the

conditons in the antimicrobial activity testing where the particles did not cover the titanium plates. The pH of the SBF was measured in triplicates at 37ºC with at 2, 10, 30, 60 and 120min.

For the dynamic dissolution tests, fresh SBF at 37ºC was continuously fed at 0.2 mL/min through a bed of glass particles (285 mg, 300-500μm) using the method described in detail by Fagerlund et al. (2012, 2013) [37,38]. The solution was collected at selected time points for 15 min after which the ion concentrations released from the glass particles was measured using ICP-OES. The measurements were continued up to 50 hrs, i.e. to a time point at which the antibacterial effect and biofilm growth inhibiting effect of a particular composition can be distinguished [20,21,34].

Substrates and surface treatment

Sixty five commercially pure titanium discs grade-1 (diameter 10 mm and thickness 1 mm) were polished with 1200-, 2400-, and 4000- grit silicon carbide (SiC) papers. Then the titanium discs were cleaned in an ultrasonic bath, containing acetone, for 10 min. The titanium discs were rinsed in double distilled water and dried at room temperature. Air-abrasive device (LM ProPower, Parainen, Finland) was used to air abrade the titanium disc surfaces with the glass particles as specified above. The air abrasion procedure using BAG particles (Zn4, Zn6, Zn4Sr8, 45S5 and E-glass) was performed from a distance of 3 mm for 20 sec using 4 bars air pressure in 90° angle.

The retention of glass particles on the titanium discs was evaluated from SEM-EDS (LEO Gemini 1530 with a Thermo Scientific UltraDry Silicon Drift Detector) analyses of

the same areas of disc surfaces before and after 15 min using of ultrasonic bathing in water.

Antimicrobial activity test

The capability of the BAG abraded titanium discs to prevent microorganism growth was studied for samples exposed to air-particle abrasion. In all experiments the microorganism used was *Streptococcus mutans* Ingbritt. It was first grown overnight in Brain Heart Infusion medium (BHI; Becton-Dickinson and Company, Sparks, MD, USA), then transferred to fresh medium and grown until log-phase. Then the cells were suspended in fresh BHI, A550 = 0.35. Twelve µl of this suspension was pipetted on the BAG abraded titanium discs inserted in 24-well cell culture plates. Each titanium disc was covered with a piece of Mylar film (Etra Oy, Helsinki, Finland), the size being equal to the disc (10x10 mm). The culture plates were incubated in an anaerobic chamber (Don Whitley Scientific LTD., Shipley, UK; 80% N_2, 10% CO_2, 10% H_2) at +37 ˚C for 4 h. After the incubation, the titanium discs and films were placed in 1 ml phosphate-buffered saline. The viable cells from the discs were collected with microbrushes (Quick-Stick, Dentsolv AB, Saltsjö-Boo, Sweden) and dispersed with mild sonication. The suspensions containing the bacteria were serially diluted and plated on Mitis Salivarius Agar (Becton-Dickinson and Company). The Agar plates were grown for 3 days anaerobically at +37 ˚C. The colonies were counted under a stereomicroscope and results expressed as colony-forming units (CFU). The experiments were performed with 4 replicates and repeated at least once.

Biofilm experiments

For the biofilm experiments *S. mutans* Ingbritt grown in BHI as described above. After washing, the cells were suspended in BHI containing 1% sucrose (A550 = 0.05). This suspension was further diluted 1:50 and 2 ml was pipetted onto the BAG abraded titanium discs placed in 24-well culture plates. The plates were incubated anaerobically for 24 h at 37 ˚C. The collection of the biofilm and culturing of cells was performed as described above. The method has been described in detail earlier [39]. The experiments were performed with 4 replicates and repeated at least once.

Adhesion test

For the cell adhesion tests, *S. mutans* Ingbritt was grown overnight in BHI, washed once (5 000 x*g*, 10 min) in saline, and suspended in saline, A550 = 0.35. Due to the potential surface activity of air-particle abraded discs they were used in the experiments without presoaking or precoating. The procedure has been described in detail in Lassila et al. [40] In short, the BAG abraded titanium discs were rolled in the cell suspensions for 30 min, washed three times in saline, after which the cells were scraped from the disc surfaces with applicators. The brush ends of the applicators were cut into 0.5 ml transport medium (Tryptic Soy Broth, Becton-Dickinson and Company) and the suspensions were cultured as described above. This cell collection method has been tested earlier and it is highly reproducible [40,41]. The experiments were performed with 5 replicates and repeated at least once.

Statistical analysis

For description of the data, mean values and SDs were calculated. Statistical analysis were conducted using SPSS (version 23.0; SPSS. Inc, Chicago, IL, UAS). One-way ANOVA followed by Tukey's 'post-hoc were used to determine if there were significant differences between each experimental treatment with a p value of <0.05.

RESULTS

SEM-EDS analysis of the titanium discs air-abraded with BAG particles demonstrated that BAG particles were strongly attached to the titanium disc surfaces. The ultrasonic bath for the titanium discs air-abraded with BAGs/E-glass for 15 min had no effect on the amount of glass particles attached to the titanium surfaces (for titanium abraded with the 45S5 BAG, see Fig. 1).

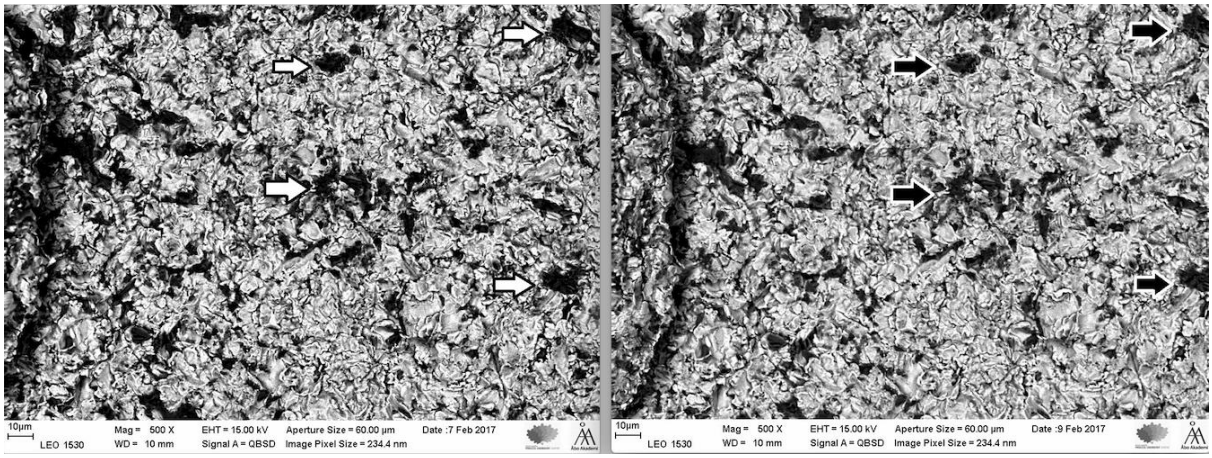

Fig. 1 *SEM images of 45S5 BAG air-abraded titanium discs at 600x magnification. A: BAG particles on the discs after air-particle abrasion process; B: the same area after 15 minutes in ultrasonic bath. Arrows show BAG particles on the discs (white arrows before ultrasonic bath and black arrows after the ultrasonic bath.)*

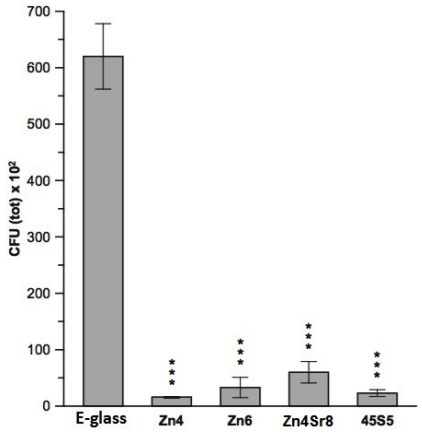

Fig. 2 *Viable S. mutans on BAGs/ E-glass air-particle abraded titanium discs. Statistical significance, ***p<0.001.*

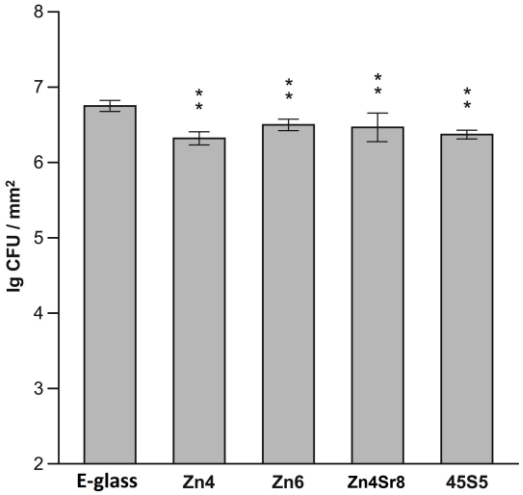

Fig. 3 *S. mutans biofilm formation on BAG/ E-glass air-particle abraded titanium discs. Statistical significance, **p<0.01.*

A more than a ten-fold decrease in the viability of *S. mutans* was observed for titanium discs air-abraded with the BAGs compared to E-glass control ($p<0.001$). (Fig. 2). Based on the mean values, there was a tendency for Zn4 to have a higher antimicrobial effect than the other Zn-containing BAGs, however, this difference was not statistically significant.

Also a significant decrease in biofilm formation was observed for all BAGs compared to E-glass ($p<0.01$; Fig. 3). No significant differences were seen between BAGs. However, adhesion of *S. mutans* was similar to all titanium surfaces air-abraded with the BAGs vs. E-glass (Fig. 4).

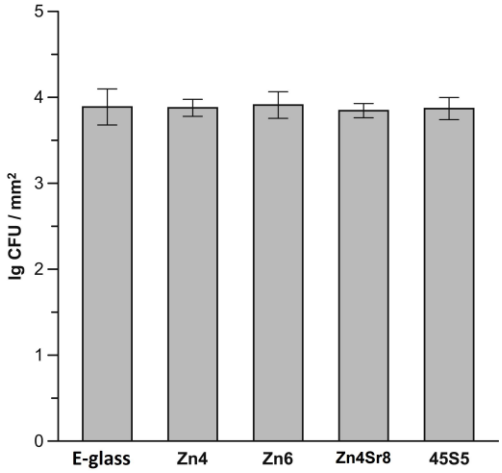

Fig. 4 *Adhesion of S. mutans to BAGs/ E-glass air-particle abraded titanium discs. No statistical significances were detected.*

Table 2. Average concentrations of ions (mg/L) released into SBF from the experimental glasses and 45S5 in continuous flow and in static conditions. The values for the continuous flow conditions are for the solution gathered from the outlet of the glass sample for 15 min at the time points starting at 2 and 48 hrs. The values for the static system are for the total solution after 48 hrs. The relative standard deviation of the concentrations of each element is around 5%.

Glass code	Si (mg/L)			Ca (mg/L)			Zn (mg/L)			Sr (mg/L)		
	Continuous flow		Stat.	Cont. flow		Stat.	Cont. flow		Stat.	Cont. flow		Stat.
	2 h	48 h	48 h	2 h	48 h	48 h	2 h	48 h	48 h	2 h	48 h	48 h
45S5	41	16	58	126	66	200	-	-	-			
Zn4	5	6	30	83	70	149	0.2	0.2	0.04			
Zn6	5	6	33	85	94	152	0.01	0.05	0.06			
Zn4Sr8	9	6	37	82	67	130	0.01	0.05	0.01	7	5	68

The release of ions from the glasses was measured using two approaches: continuous flow and static conditions. In the dynamic flow conditions, fresh solution was continuously fed through the bed of the glass particles. During the first 30-60 minutes, the concentrations of ions released went through a maximum value. For 45S5, the maximum concentrations were 58 mg/L for Si and 128 mg/L for Ca. For the experimental

BAGs, the maximum ion concentrations were much lower. For all three ZnO –containing glasses the maximum concentrations were for in the range 13-17 mg/L for Si, 80-100 mg/L for Ca and less than 0.1 mg/L for Zn. After the initial peak values, the concentrations stabilized to rather constant values as seen in for 2 and 48 hrs in Table 2. The variations between these two time points are within the accuracy of the measurement. In the continuous flow measurements, the dissolution reactions of 45S5 increased the pH of the SBF from the initial value 7.40 to around 7.8 but the gradually decreased to 7.54 at 2 hours and 7.44 at 48 hours. All values are averages of three parallel measurements. In contrast, the lower ion dissolution from the experimental Zn –containing glasses gave only a slight initial increase during the first minutes: pH=7.43 for Zn4, pH=7.49 for Zn6 and pH=7.46 for Zn4Sr8. After the initial dissolution, the ion release was too low to affect the pH of the fresh buffered solution flowing through the particles of Zn4 and Zn4Sr8. At 48 hrs, the ion dissolution from Zn6 induced a minor increase, pH=7.42. The ion concentrations released into the static solution are also given in Table 2. Silicon concentration was the highest, 58 mg/mL and around the saturation limit of the solution. For all other glasses, the the Si concentration was much lower. Similar difference could also be seen for the Ca^{2+} concentration. In general, the Zn^{2+} concentrations in the soutions were low after 48 hrs while rather high concentration of Sr^{2+} was measured for Zn4Sr8. Since all the release of all elements from the BAGs was measured simultaneously, the high initial concentration of Na^{+} in the SBF made accurate predictions of its release difficult. Thus, no values for Na^{+} are shown in Table 2.

The influence of the glass particles on the solution pH in static conditions was measured at several time points (Figure 5).

45S5 and Zn6 BAGs demonstrated the highest pH increase ($p<0.001$) during the first 2 min of immersion. Thereafter the BAG 45S5 showed a linear increase in the pH and was around 9 at 120 min. The increase in the pH was significantly higher for 45S5 compared to the three Zn-containing BAGs ($p<0.001$; Fig. 5). For all Zn-containing BAGs the pH remained on a similar level after the initial increase at 2 min, however, it was at all time points significantly higher for Zn6 as compared to Zn4 and Zn4Sr8 BAGs ($p<0.001$; Fig 5).

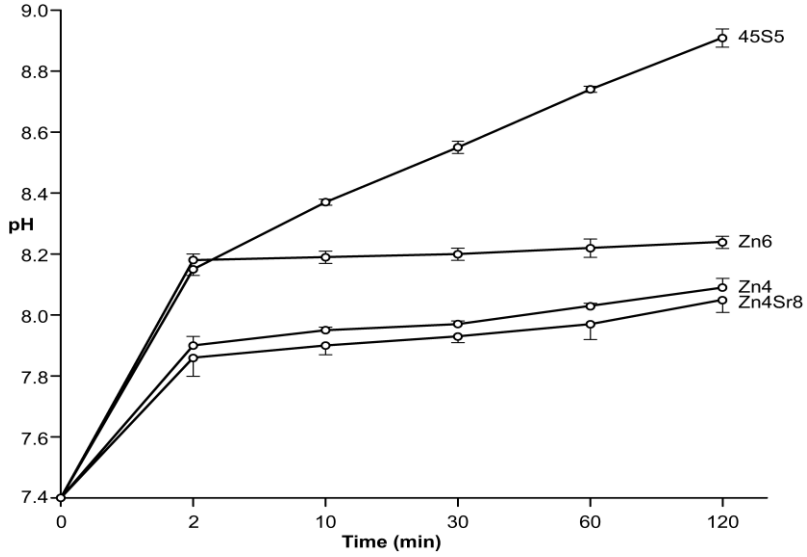

Fig. 5 *Effect of 45S5 BAG and Zn-containing BAGS on the SBF pH value during 120 min evaluations. Statistical significances; 45S5 vs Zn-containing BAGs ***p<0.001, Zn6 vs Zn4 and Zn4Sr8 ***p<0.001*

DISCUSSION

In this study, titanium air abrasion with Zn4, Zn6, Zn4Sr8 and 45S5 BAG particles exhibited antibacterial effect against *S. mutans*. Furthermore, they showed a potential ability to inhibit biofilm formation on air-abraded titanium substrates.

The dimensions of the BAG/E-glass granules used in this study ranged from 25-120μm. The air-abrasion procedure with BAG/E-glass modified significantly the titanium

surfaces and produced similar surface topographies which was confirmed by SEM. The surface topography is important since oral biofilm formation of the early colonizers, streptococci, on titanium surfaces depends on both the surface topography and species involved [42]. We chose *S. mutans* for this study because it is very virulent, forms adhesive biofilm [18], and might thus participate in the process, which can lead to implant failure [13]. *S. mutans* was found to be at higher level around infected implants than around healthy implants [9]. Furthermore, *S. mutans* is well known to have numerous efficient means of adhesion to different surfaces that enable formation of an highly adherent biofilm [14,43]. In contrast, the Gram-negative and anaerobic bacteria that are commonly associated with peri-implantitis have rather less efficient adherence mechanisms [44].

The release of alkaline ions (Na^+ and Ca^{2+}) from BAG 45S5 is high and contributes to an elevated pH in the vicinity of the dissolving glass. The rapid initital release of the alkalis is believed to be the main factor in the antimicrobial effect of BAGs towards microorganisms [18,34]. In our study, 45S5 BAG demonstrated the highest pH increase compared to the Zn-containing BAGs both in the static and continuous flow experiments. High pH has been suggested to be the possible mechanism of the antibacterial effect of 45S5 BAG particles. In the study of Allan et al. (2001) 45S5 BAG had an antibacterial effect against certain supragingival and subgingival bacteria including *S. mutans* with 83.1% of loss in viability after 1 h and 97.3 after 3 h of exposure to BAG [19]. S. mutans planktonic cells lost nearly all their activity after 10 min of contact to S53P4 BAG powder from 6 x 106 to 0.8 x 101 [18]. However, the mechanism behind the Zn-containing BAGs antibacterial effects may not be associated

with the pH changes. Zinc-containing BAGs demonstrated slight elevation of pH from 7.4 to pH = 8.1-8.2 in the static experiments. Our laboratory was the first to demonstrate the antimicrobial effects of easily soluble BAGs on oral microorganisms [18]. It should be pointed out that although the pH and ion release measurements were done using BAG particle size fractions markedly larger than those used in the air-abrasion, the trends between the different compositons can be correlated with the antibacterial effects. The ion concentrations measured at the flowing conditions give momentaneous released into the the fresh solution and typically give high initial release of silicon and calcium species from 45S5. The release rate slows down with time, partly because of the gradual development of hydroxyapatite layer on the surface of the 45S5 BAG particles. In contrast, the release of silicon, calcium, Zinc and strontium ions from the experimental glasses is clearly less and of the same level, within the accuracy of the measurements, at 2 and 48 hrs in the flowing conditions. For all glasses, the concentrations of silicon and calcium ions are clearly higher in the static conditions. For 45S5, the Si concentration is close to the saturation of the solution and the formation of the typical silica-rich and hydroxyapatite layers is likely to control the overall dissolution [17]. The static condition values for the experimental glasses are clearly lower, thus explaining the observed low pH values. Interestingly, the release of Zn^{2+} is relatively low but almost constant. Sr^{2+} release pattern can be compared with that of Ca^{2+} and the concentrations released are markedly higher than those of Zn^{2+}. Substituting larger Sr^{2+} ions for Ca^{2+} in bioactive glasses has been found to decrease the chemical durability and thus lead to easy release of Sr^{2+} to the interfacial solution [45]. The differences between the three experimental glasses can be explained by the impact of Zn^{2+} and Sr^{2+} on the glass network structure. ZnO is

classified as an intermediate oxide while SrO is a network modifier. According to Table 1, all the experimental glasses have lower theoretical network connectivity, NC, than 45S5. Accordingly, they should dissolve easier. However, all the in vitro tests show lower dissolution for the ZnO and SrO doped experimental glasses (Table 2). Considering that the NC formula for bioactive glasses by Hill and Brauer (2011) [35] does not take into account any intermediate oxides, it is likely that ZnO acts primarily as a glass network former in these compositions. In addition, Zn^{2+} released into the solution has been found to easily precipitate as $Zn_3(PO_4)_2{\cdot}4H_2O$ and $Zn(OH)_2$ [46,47]. The easy precipitation of Zn salts also explains that the pH of SBF is low in static conditions and in continuous flow conditions at longer time points is slightly below the original value. Whether the precipitation of Zn salt species forms a dissolution barrier at the glass surface should be verified with additional experiments. The slightly higher release of Si, Ca and other species for Zn6 compared to Zn4 and Zn4Sr8 can be correlated with its lower network connectivity (Table 1). Differences between Zn4 and ZnSr8 with the same theoretical network connectivity again are likely due to the bigger size and thus weaker bonding strength of Sr^{2+} compared to Ca^{2+} in Zn4Sr8. The steady release of Zn^{2+} in the dynamic flow conditions especially for Zn4 BAG composition suggests that before any precipitation, the Zn ion concentration is relatively high in the interfacial solution. The ion release concentrations in the dynamic flow conditons were thus assumed to correlate with the observed antibacterial effects of the BAG abraded titanium discs.

The dissolving Zn^{2+} ions apparently were involved in the antibacterial activity since Zn^{2+} ions can penetrate the bacterial cell and produce toxic reactive oxygen species (ROS) which cause DNA and cell membrane damage [23]. In our study, Zn4 BAG illustrated the highest Zn^{2+} ion release resulting in the concentration of 0.2 mg/L in 2 h and 48 h compared to Zn6 and Zn4Sr8 BAGs (0.01-0.05 mg/L). Ning et al. (2015) reported that the minimum inhibitory concentration (MIC) of Zn^{2+} ions was 10^{-7} M (0.0065 mg/L) and the optimal concentration range of Zn^{2+} ions that have antimicrobial activity without cytotoxity was 10^{-4} – 10^{-6} M (6.53 - 0.065 mg/L) [48].

In accordance with the antimicrobial activity tests all BAGs inhibited S. *mutans* biofilm formation. This is also supporting the idea that the topographies of the discs were similar, since topography affects *S. mutans* biofilm formation on titanium surfaces [34]. The biofilm inhibition is for 45S5 BAG most probably due to the increase in the pH and for Zn-containing BAGs it is the release of Zn^{2+} ions as discussed above. The tissue-friendly Zn^{2+} may be of benefit for the healing process [49], compared to the 45S5 BAG, causing a strong elevation of pH in its vicinity. *S. mutans* showed similar adhesion to all abraded titanium alloy discs which is in accordance with the similar topographies of the discs. The adhesion experiments were performed in conditions which prevent local effects like pH or Zn^{2+} ion concentration increases, thus the surface topography as well as surface energy should influence adhesion of *S. mutans*. However, the *S. mutans* viability and biofilm inhibition results are not related to the adhesion.

SUMMARY AND CONCLUSIONS

We showed that titanium alloy discs abraded with three ZnO and SrO doped 45S5 BAGs had strong antimicrobial activity against *S. mutans* and they suppressed *S. mutans* biofilm formation. This effect was not related to the adhesion of *S. mutans* to the discs. The antimicrobial activity was for 45S5 BAG most probably due to the high pH and for the Zn-containing BAGs the steady release of Zn^{2+} in critical concentrations. Addition of ZnO was found to increase the antibacterial properties of 45S5 BAG. Zn4 BAG is believed to be the most applicable among the three Zn containing BAGs due to the fact that the release of Zn ions is relatively large and stable.

CONFLICTS OF INTEREST

The authors of the present article would like to declare no conflicts of interest with regard to the information found in the presented work

References

1. Aglietta M, Siciliano VI, Zwahlen M, et al. A systematic review of the survival and complication rates of implant supported fixed dental prostheses with cantilever extensions after an observation period of at least 5 years. *Clin Oral Implants Res*. 2009;20(5):441-451.

2. Ong CT, Ivanovski S, Needleman IG, et al. Systematic review of implant outcomes in treated periodontitis subjects. *J Clin Periodontol*. 2008;35(5):438-462.

3. Tonetti MS. Risk factors for osseodisintegration. *Periodontol 2000*. 1998;17:55-62.

4. Lang NP, Wilson TG, Corbet EF. Biological complications with dental implants: Their prevention, diagnosis and treatment. *Clin Oral Implants Res*. 2000;11 Suppl 1:146-155.

5. Mombelli A, van Oosten MA, Schurch E,Jr, Land NP. The microbiota associated with successful or failing osseointegrated titanium implants. *Oral Microbiol Immunol*. 1987;2(4):145-151.

6. Zitzmann NU, Berglundh T. Definition and prevalence of peri-implant diseases. *J Clin Periodontol*. 2008;35(8 Suppl):286-291.

7. Heitz-Mayfield LJ, Lang NP. Comparative biology of chronic and aggressive periodontitis vs. peri-implantitis. *Periodontol 2000*. 2010;53:167-181.

8. Shibli JA, Martins MC, Lotufo RF, Marcantonio E,Jr. Microbiologic and radiographic analysis of ligature-induced peri-implantitis with different dental implant surfaces. *Int J Oral Maxillofac Implants*. 2003;18(3):383-390.

9. Kumar PS, Mason MR, Brooker MR, O'Brien K. Pyrosequencing reveals unique microbial signatures associated with healthy and failing dental implants. *J Clin Periodontol*. 2012;39(5):425-433.

10. Shibli JA, Vitussi TR, Garcia RV, et al. Implant surface analysis and microbiologic evaluation of failed implants retrieved from smokers. *J Oral Implantol*. 2007;33(4):232-238.

11. Shibli JA, Melo L, Ferrari DS, Figueiredo LC, Faveri M, Feres M. Composition of supra- and subgingival biofilm of subjects with healthy and diseased implants. *Clin Oral Implants Res*. 2008;19(10):975-982.

12. Kuramitsu HK, He X, Lux R, Anderson MH, Shi W. Interspecies interactions within oral microbial communities. *Microbiol Mol Biol Rev*. 2007;71(4):653-670.

13. Nakazato G, Tsuchiya H, Sato M, Yamauchi M. In vivo plaque formation on implant materials. *Int J Oral Maxillofac Implants*. 1989;4(4):321-326.

14. Koo H, Falsetta ML, Klein MI. The exopolysaccharide matrix: A virulence determinant of cariogenic biofilm. *J Dent Res*. 2013;92(12):1065-1073.

15. Tamura S, Yonezawa H, Motegi M, et al. Inhibiting effects of streptococcus salivarius on competence-stimulating peptide-dependent biofilm formation by streptococcus mutans. *Oral Microbiol Immunol*. 2009;24(2):152-161.

16. Hench LL, Paschall HA. Direct chemical bond of bioactive glass-ceramic materials to bone and muscle. *J Biomed Mater Res*. 1973;7(3):25-42.

17. Hench LL. Bioactive ceramics. *Ann N Y Acad Sci*. 1988;523:54-71.

18. Stoor P, Soderling E, Salonen JI. Antibacterial effects of a bioactive glass paste on oral microorganisms. *Acta Odontol Scand*. 1998;56(3):161-165.

19. Allan I, Newman H, Wilson M. Antibacterial activity of particulate bioglass against supra- and subgingival bacteria. *Biomaterials*. 2001;22(12):1683-1687.

20. Munukka, E., Leppäranta, O., Korkeamäki, M., Vaahtio, M., Peltola,T., Zhang, D., Hupa, L., Ylänen, H., Salonen, J., Viljanen, M.K., Eerola, E., Bactericidal effects of bioactive glasses on clinically important aerobic bacteria. Journal of Materials Science: Materials in Medicine, 19(1) (2008) 27-32.

21. Leppäranta, O., Vaahtio, M., Peltola, T., Zhang, D., Hupa, L., Hupa, M., Ylänen, H., Salonen, J.I., Viljanen, M.K., Eerola, E. Antibacterial effect of bioactive glasses on clinically important anaerobic bacteria in vitro. Journal of Materials Science: Materials in Medicine, 19(2) (2008) 547-551.

22. Allan I, Newman H, Wilson M. Particulate bioglass reduces the viability of bacterial biofilms formed on its surface in an in vitro model. *Clin Oral Implants Res*. 2002;13(1):53-58.

23. Yamamoto O. Influence of particle size on the antibacterial activity of zinc oxide. *International Journal of Inorganic Materials*. 2001;3(7):643-646.

24. Sawai J, Shoji S, Igarashi H, et al. Hydrogen peroxide as an antibacterial factor in zinc oxide powder slurry. *Journal of Fermentation and Bioengineering*. 1998;86(5):521-522. doi: http://dx.doi.org/10.1016/S0922-338X(98)80165-7.

25. Mohd Bakhori SK, Mahmud S, Ling CA, et al. In-vitro efficacy of different morphology zinc oxide nanopowders on streptococcus sobrinus and streptococcus mutans. *Materials Science and Engineering: C*. 2017;78:868-877.

26. Ishikawa K, Miyamoto Y, Yuasa T, Ito A, Nagayama M, Suzuki K. Fabrication of zn containing apatite cement and its initial evaluation using human osteoblastic cells. *Biomaterials*. 2002;23(2):423-428.

27. Collier FM, Huang WH, Holloway WR, et al. Osteoclasts from human giant cell tumors of bone lack estrogen receptors. *Endocrinology*. 1998;139(3):1258-1267.

28. Wang N, Li H, Lu W, et al. Effects of TiO2 nanotubes with different diameters on gene expression and osseointegration of implants in minipigs. *Biomaterials*. 2011;32(29):6900-6911.

29. Zhang W, Li Z, Liu Y, et al. Biofunctionalization of a titanium surface with a nano-sawtooth structure regulates the behavior of rat bone marrow mesenchymal stem cells. *Int J Nanomedicine*. 2012;7:4459-4472.

30. Yeo IS. Reality of dental implant surface modification: A short literature review. *Open Biomed Eng J*. 2014;8:114-119.

31. van Velzen FJ, Ofec R, Schulten EA, Ten Bruggenkate CM. 10-year survival rate and the incidence of peri-implant disease of 374 titanium dental implants with a SLA surface: A prospective cohort study in 177 fully and partially edentulous patients. *Clin Oral Implants Res*. 2015;26(10):1121-1128.

32. Liu, J., Rawlinson, S.C., Hill, R.G., Fortune, F., Strontium-substituted bioactive glasses in vitro osteogenic and antibacterial effects. Dental Materials 2016, 32 (3), 412-422.

33. Balasubramanian, P., Strobel, L.A., Kneser, U., Boccaccini, A.R. Zinc-containing bioactive glasses for bone regeneration, dental and orthopedic applications. Biomed. Glasses 2015; 1:51–69.

34. Zhang D, Lepparanta O, Munukka E, et al. Antibacterial effects and dissolution behavior of six bioactive glasses. *J Biomed Mater Res A*. 2010;93(2):475-483.

35. Hill, R.G., Brauer, D.S. Predicting the bioactivity of glasses using the network connectivity of split network models. Journal of Non-Crystalline Solids, 357 (2011) 3884-3887.

36. Kokubo T, Kushitani H, Sakka S, Kitsugi T, Yamamuro T. Solutions able to reproduce in vivo surface-structure changes in bioactive glass-ceramic A-W. *J Biomed Mater Res*. 1990;24(6):721-734.

37. Fagerlund, S., Ek, P., Hupa, M., Hupa, L. Dissolution kinetics of a bioactive glass by continuous measurement. Journal of the American Ceramic Society, 95(10) (2012) 3130-3137.

38. Fagerlund, S., Hupa, L., Hupa, M. Dissolution patterns of biocompatible glasses in 2-amino-2-hydroxymethyl-propane-1,3-diol (Tris) buffer, Acta Biomaterialia, 9(2) (2013) 5400-10.

39. Liang X, Soderling E, Liu F, He J, Lassila LV, Vallittu PK. Optimizing the concentration of quaternary ammonium dimethacrylate monomer in bis-GMA/TEGDMA dental resin system for antibacterial activity and mechanical properties. *J Mater Sci Mater Med*. 2014;25(5):1387-1393.

40. Lassila LV, Garoushi S, Tanner J, Vallittu PK, Soderling E. Adherence of streptococcus mutans to fiber-reinforced filling composite and conventional restorative materials. *Open Dent J*. 2009;3:227-232.

41. Tanner J, Robinson C, Soderling E, Vallittu P. Early plaque formation on fibre-reinforced composites in vivo. *Clin Oral Investig*. 2005;9(3):154-160.

42. Nascimento C, Pita MS, Santos Ede S, et al. Microbiome of titanium and zirconia dental implants abutments. *Dent Mater*. 2016;32(1):93-101.

43. Hamada S, Slade HD. Biology, immunology, and cariogenicity of streptococcus mutans. *Microbiol Rev*. 1980;44(2):331-384.

44. Nobbs AH, Jenkinson HF, Jakubovics NS. Stick to your gums: Mechanisms of oral microbial adherence. *J Dent Res*. 2011;90(11):1271-1278.

45. Hupa, L, Fagerlund, S , Massera, J & Björkvik, L 2016, ' Dissolution behavior of the bioactive glass S53P4 when sodium is Replaced by potassium, and calcium with magnesium or strontium " *Journal of Non-Crystalline Solids* , Pages 41-46 . DOI: 10.1016 / j.jnoncrysol.2015.03.026

46. Du R.L., Chang J., Ni S.Y., Zhai W.Y., Wang J.Y., Characterization and in vitro bioactivity of zinc-containing bioactive glass and glass-ceramics, J. Biomater. Appl. 2006, 20, 341–360

47. Balamurugan A., Balossier G., Kannan S., Michel J., Rebelo A.H.S., Ferreira J.M.F., Development and in vitro characterization of sol-gel derived CaO-P2 O5 -SiO2 -ZnO bioglass, Acta Biomater. 2007, 3, 255–262

48. Ning C, Wang X, Li L, et al. Concentration ranges of antibacterial cations for showing the highest antibacterial efficacy but the least cytotoxicity against mammalian cells: Implications for a new antibacterial mechanism. *Chem Res Toxicol*. 2015;28(9):1815-1822.

49. Kogan S, Sood A, Garnick MS. Zinc and wound healing: A review of zinc physiology and clinical applications. *Wounds*. 2017;29(4):102-106.